Appl. Phys. B (2013) 112:457–460
DOI 10.1007/s00340-013-5526-y

Applied Physics B
Lasers and Optics

RAPID COMMUNICATION

Nonlinear optics in Xe-filled hollow-core PCF in high pressure and supercritical regimes

M. Azhar · N. Y. Joly · J. C. Travers · P. St. J. Russell

Received: 6 May 2013 / Accepted: 21 May 2013 / Published online: 30 May 2013

Abstract Supercritical Xe at 293 K offers a Kerr nonlinearity that can exceed that of fused silica while being free of Raman scattering. It also has a much higher optical damage threshold and a transparency window that extends from the UV to the infrared. We report the observation of nonlinear phenomena, such as self-phase modulation, in hollow-core photonic crystal fiber filled with supercritical Xe. In the subcritical regime, intermodal four-wave mixing resulted in the generation of UV light in the HE_{12} mode. The normal dispersion of the fiber at high pressures means that spectral broadening can be clearly obtained without influence from soliton effects or material damage.

The long diffraction-free interaction lengths provided by hollow-core photonic crystal fiber (HC-PCF) make it uniquely versatile for the study of nonlinear optics in gases, offering a high damage threshold and orders of magnitude lower transmission loss compared to capillaries of the same ($\sim$20 μm) core diameter [1, 2]. A special subclass of these fibers is kagomé-style HC-PCF, which provides ultra-broadband optical transmission at losses below $\sim$2 dB/m, the guidance mechanism being a form of two-dimensional anti-resonant reflection [3]. In addition, when evacuated, kagomé-PCF has weak and smoothly wavelength-dependent anomalous dispersion that can be balanced against the normal dispersion of a filling gas, permitting the dispersion landscape to be pressure-tuned. In previous work on Ar-filled kagomé-PCF, this enabled observation of tunable deep-UV (DUV) light via dispersive wave generation from self-compressed fs pulses at 800 nm [4] and the first observation of a plasma-driven soliton blue-shift [6, 6]. Noble gas-filled capillaries [7–9] and photonic bandgap HC-PCFs [10] have been used for pulse compression where the nonlinearity of the gas was used to broaden the spectrum of the launched pulse. Xe-filled kagome-lattice [11] has also been used for pulse compression at low pressures. Corkum et al. [12] observed self-focusing-induced supercontinuum generation in bulk gaseous Xe.

In this paper, we report on ultrafast nonlinear dynamics in kagomé-PCF filled with high pressure and supercritical Xe. Previous studies of supercritical gases have included Brillouin scattering in Xe [13] and Raman scattering in CO_2 [14]. Using tabulated density data at ambient temperature (293 K) [15], the n_2 values for Ar, Kr and Xe are plotted against pressure in Fig. 1a, assuming that n_2 is proportional to density. Note that the critical points are (48 bar, $\sim$150 K) for Ar, (55 bar, $\sim$209 K) for Kr and (58 bar, $\sim$289 K) for Xe. At room temperature, the influence of the critical point is weak for Kr and Ar, and therefore, the gas density, and hence n_2, varies more or less linearly with pressure, reaching, respectively, $\sim$5 and $\sim$23 % of the value in fused silica glass at 150 bar [16].

For Xe, the influence of the critical point is much stronger, leading to a sharp increase in n_2 when the pressure reaches $\sim$60 bar [15]; recent linear measurements have confirmed this [17]. When the pressure and temperature lie above the critical point—easily achievable in experiment without the need for a cryogenic system [18]—Xe becomes a supercritical fluid, with a nonlinearity that can exceed that of fused silica.

M. Azhar (✉) · N. Y. Joly · J. C. Travers · P. St. J. Russell
Max Planck Institute for the Science of Light,
Günther-Scharowsky-Str. 1, 91058 Erlangen, Germany
e-mail: mohiudeen.azhar@mpl.mpg.de

N. Y. Joly · P. St. J. Russell
Department of Physics, University of Erlangen-Nuremberg,
Günther-Scharowsky-Str. 1, 91058 Erlangen, Germany

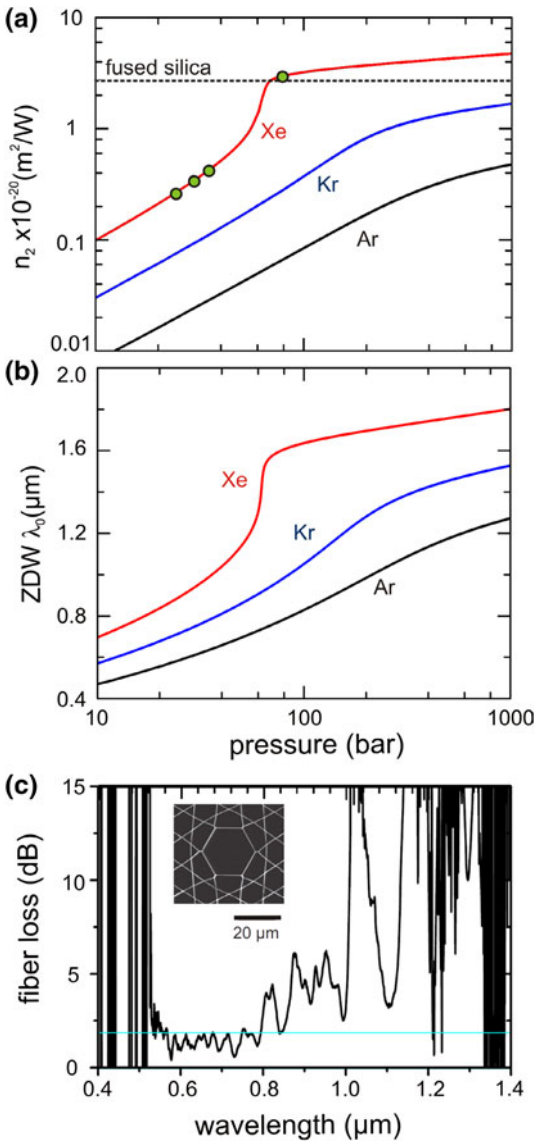

Fig. 1 **a** The dependence of nonlinearity n_2 on pressure at 293 K for Xe, Kr and Ar. The nonlinearity of fused silica is included for comparison. For Xe, the curve starts out linear and then sharply increases close to the critical point. The green circles mark the pressures at which the experiments were performed. **b** Pressure-dependence of the zero dispersion wavelength in a gas-filled kagomé-PCF with a core diameter of 18 μm. The dispersion is anomalous for wavelengths longer than λ_0. **c** Fiber loss, illustrating the broad transmission range of the kagomé-PCF used. The inset is a scanning electron micrograph of the fiber structure

Theory predicts that Xe will exhibit a temporally non-local (response times in the μsec range) nonlinearity close to the critical point [19], due to intense scattering arising from critical opalescence. In this paper, we avoid this regime by operating sufficiently above or below the critical point, where Xe remains transparent.

As described in previous papers, the dispersion of the guided mode in kagomé-PCF can be described using a capillary model [20, 21]. As the pressure increases, the normal dispersion of the gas counteracts the weak anomalous waveguide dispersion of the empty kagomé PCF, creating a pressure-tunable zero dispersion wavelength (ZDW, λ_0). Figure 1b shows the variation of λ_0 with pressure for Ar, Kr and Xe. Although Xe clearly extends the range of tunability of λ_0 compared to Ar and Kr, opalescence makes it unusable in the vicinity of the supercritical transition. Note that the dispersion can also be tuned by changing the fiber core diameter; for example, λ_0 could be shifted further into the infrared with larger core diameters [2]. At pressures larger than 15 bar, the dispersion becomes normal for the pump wavelength of 800 nm, enabling the observation of effects such as intermodal four-wave mixing (iFWM) [22] without interference from soliton dynamics, which usually dominates in the anomalous dispersion region.

The experimental set-up consisted of a 28 cm length of kagomé-PCF (core diameter 18 μm) with a high-pressure gas cell at each end. The pump laser was an amplified Ti : sapphire system (wavelength 800 nm) delivering pulses of duration 150 fs and energy $\sim$1.8 μJ at a repetition rate of 250 kHz. Diagnostics included a UV-sensitive camera for modal imaging and a spectrometer sensitive from 200 to 1100 nm. To prevent the spectrometer from saturating, the signal was attenuated by reflection at two wedged glass plates. A parabolic mirror was then used to focus light into the spectrometer.

Supercritical Xe was collected by liquefying Xe in steel pipes cooled by dry ice. After a sufficient amount of Xe had collected, the pipes were warmed up to room temperature. This simple procedure allowed us to reach Xe pressures of 200 bar from a 40 bar gas cylinder while maintaining high Xe purity.

We filled the fiber with Xe at 80 bar, placing it well inside the supercritical regime at 293 K. At this pressure, the nonlinear refractive index is $\sim 2.8 \times 10^{-20}$ m^2/W [23, 24], which matches the value for fused silica [25] (Fig. 1a). It can be seen from Fig. 1a that Ar and Kr do not reach this level of nonlinearity even at pressures of 1000 bar. Supercritical Xe on the other hand exceeds the nonlinearity of fused silica even at 100 bar. As the launched pulse energy was increased, self-phase modulation (SPM) caused spectral broadening (Fig. 2). This continued up to $\sim$80 nJ, when the broadening abruptly collapsed, a dramatic effect caused by disruption of the in-coupling due to self-focusing effects in the input gas cell. To verify this, we performed experiments in a simple gas cell, obtaining reasonable agreement with full spatiotemporal numerical simulations using the methods described in [26], and simple numerical estimates of nonlinear focusing described in [27]. The self-focusing effect on fiber coupling will be further investigated.

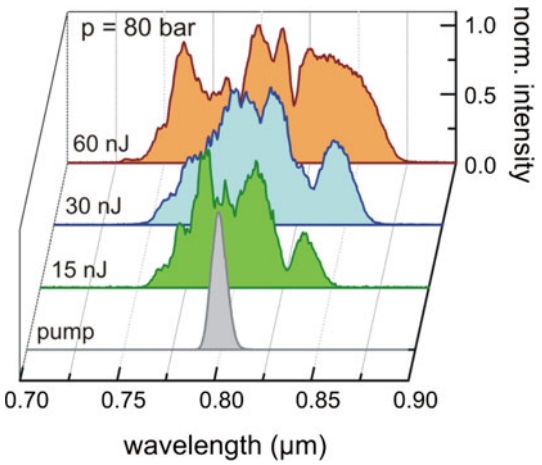

Fig. 2 Experimental output spectra (a) spectral broadening due to SPM in supercritical Xe at 80 bar for pulse energies in the fiber 15, 30 and 60 nJ

The disruptive effects of self-focusing are more apparent in the subcritical regime (Fig. 3a), where spectral broadening is abruptly attenuated above a certain critical launched energy (marked by the red arrows in Fig. 3a) that depends inversely on the pressure. This spectral collapse is accompanied by a 70 % drop in transmitted power and its threshold energy clearly drops with increasing pressure and nonlinearity (Fig. 3a). At 25 bar, $\lambda_0 \sim 890$ nm and the pump wavelength lie in the normal dispersion regime. In addition to SPM-induced spectral broadening, an unexpected band of UV light appears at ~ 330 nm. Using a narrow-band filter to isolate the near-field pattern at this wavelength (Fig. 3c), we were able to identify this signal as being in the HE_{12} mode. We attribute its appearance to intermodal four-wave mixing (iFWM). Figure 3b shows the results of a phase-matching analysis, based on the Marcatili model [20], assuming that pump and idler are in the HE_{11} mode and signal in the HE_{12} mode. As the spectrum broadens, it reaches beyond 1 μm wavelength and is then able to act as an HE_{11} idler seed for iFWM, pumped by the green spectral edge at ~ 550 nm. These two signals result in the generation, via iFWM, of signal photons in the HE_{12} mode at ~ 375 nm. The analytical theory predicts wavelengths that are in good agreement with the observations; the slight disparity between theory and experiment can be attributed to deviations of the actual fiber dispersion curve from that predicted by the Marcatili model. As a final verification, experiments in a bulk Xe cell were performed in the absence of a fiber and no iFWM was observed.

In conclusion, clear SPM broadening is observed in a HC-PCF filled with supercritical Xe, which at 80 bar has the same Kerr nonlinearity as silica. As a result of self-focusing effects in the launching cell, the spectral broadening was observed to collapse abruptly at a critical energy

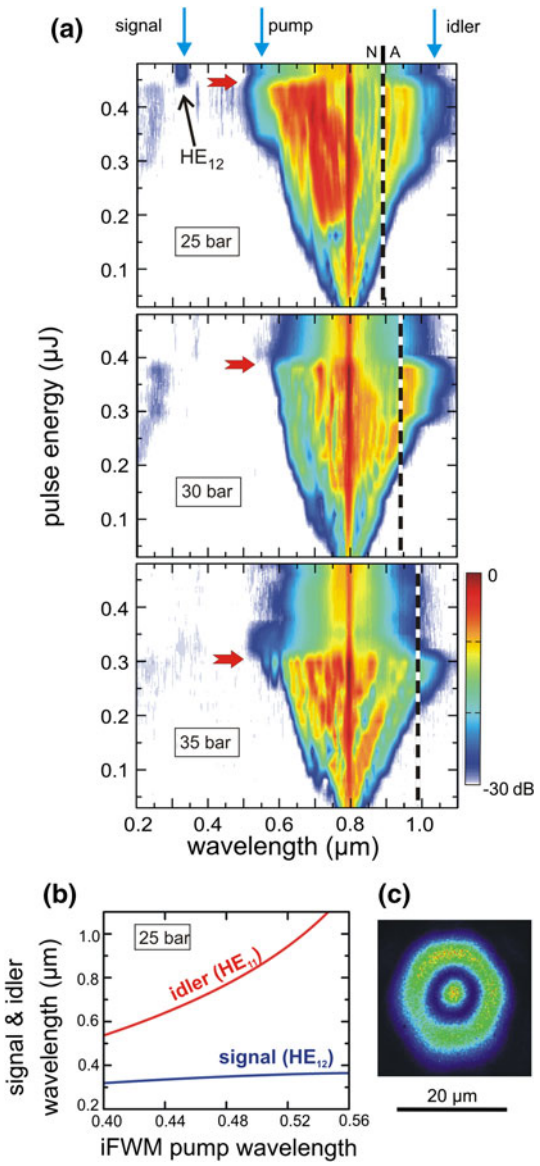

Fig. 3 **a** Experimental spectral broadening with launched pulse energy at 25 bar, 30 bar and 35 bar; the *dashed vertical lines* indicate the position of λ_0 (N = normal, A = anomalous); the *red arrows* indicate the onset of self-focusing in the input cell. **b** Theoretical phase-matching wavelengths ($2/\lambda_P = 1/\lambda_S + 1/\lambda_I$) for iFWM at 25 bar; for a ~ 550 nm pump, the signal and idler wavelengths are ~ 375 and ~ 1037 nm. The slight disagreement between theory (~ 375 nm) and experiment (signal ~ 330 nm) can be attributed to deviations of the actual fiber dispersion curve from that predicted by the Marcatili model. **c** Experimental near-field image of the light emitted in the HE_{12} mode at ~ 330 nm (the *black arrow* in **a**)

level that scaled inversely with the gas pressure; this effect could be eliminated by placing the glass window closer to the fiber end-face. Intermodal four-wave mixing was observed at 25 bar (subcritical/gaseous Xe) resulting in generation of UV light in the HE_{12} mode. Compared to all-silica fiber systems, noble gas-filled HC-PCF offers a much

higher damage threshold, excellent transparency at ultraviolet wavelengths, a low and smooth dispersion that encourage phase-matching processes, pressure-tunable dispersion and Raman-free operation. The result is a remarkably flexible system for nonlinear fiber optics.

References

1. P.St.J. Russell, J. Lightwave Technol. **24**, 4729–4749 (2006)
2. J.C. Travers, W. Chang, J. Nold, N.Y. Joly, P.St.J. Russell, J. Opt. Soc. Am. B **28**, A11–A26 (2011)
3. J.L. Archambault, R.J. Black, S. Lacroix, J. Bures, J. Lightwave Tech. **11**, 416–423 (1993)
4. N.Y. Joly, J. Nold, W. Chang, P. Holzer, A. Nazarkin, G.K.L. Wong, F. Biancalana, P.St.J. Russell, Phys. Rev. Lett. **106**, 203901 (2011)
5. P. Hölzer, W. Chang, J.C. Travers, A. Nazarkin, J. Nold, N.Y. Joly, M.F. Saleh, F. Biancalana, P.St.J. Russell, Phys. Rev. Lett. 107, 203901 (2011)
6. M.F. Saleh, W. Chang, P. Hölzer, A. Nazarkin, J.C. Travers, N.Y. Joly, P.St.J. Russell, F. Biancalana, Phys. Rev. Lett. **107**, 203902 (2011)
7. M. Nisoli, S. De Silvestri, O. Svelto, R. Szipöcs, K. Ferencz, C. Spielmann, S. Sartania, F. Krausz, Opt. Lett. **22**, 522–524 (1997)
8. A. Suda, M. Hatayama, K. Nagasaka, K. Midorikawa, Appl. Phys. Lett. **86**, 111116 (2005)
9. S. Hädrich, H. Carstens, J. Rothhardt, J. Limpert, A. Tünnermann, Opt. Exp. **19**, 7546–7552 (2011)
10. D.G. Ouzounov, C.J. Hensley, A.L. Gaeta, N. Venkateraman, M.T. Gallagher, K.W. Koch, Opt. Exp. **13**, 6153–6159 (2005)
11. O.H. Heckl, C.J. Saraceno, C.R.E. Baer, T. Südmeyer, Y.Y. Wang, Y. Cheng, F. Benabid, U. Keller, Opt. Exp. **19**, 19142–19149 (2011)
12. P.B. Corkum, C. Rolland, T. Srinivasan-Rao, Phys. Rev. Lett. **57**, 2268–2271 (1986)
13. D. Eden, H.L. Swinney, Opt. Commun. **10**, 191–194 (1974)
14. S. Howdle, K. Stanley, V. Popov, V. Bagratashvili, Appl. Spectr. **48**, 167–278 (1994)
15. E. W. Lemmon, M. O. McLinden, D. G. Friend, in NIST Chemistry WebBook, NIST Standard Reference Database No. 69, Eds. P. J. Linstrom and W. G. Mallard, National Institute of Standards and Technology, http://webbook.nist.gov
16. M. Azhar, G.K.L. Wong, W. Chang, N.Y. Joly, P.St.J. Russell, Opt. Exp. **21**, 4405–4410 (2013)
17. K.E. Lynch-Klarup, E. Mondloch, M. Raymer, F. Benabid, F. Gerome, D. Arrestier, in Frontiers in Optics conf., OSA Technical Digest (online) (Optical Society of America, 2012), paper FM4I.2
18. M. Azhar, G.K.L. Wong, W. Chang, N.Y. Joly, P.St.J. Russell, in CLEO: Science and Innovations, OSA Technical Digest (online) (Optical Society of America, 2012), paper CTh4B.4
19. R. McGraw, Phys. Rev. A **42**, 2235–2247 (1990)
20. E. Marcatili, R. Schmeltzer, Bell Syst. Tech. J. **43**, 1783–1809 (1964)
21. J. Nold, P. Hölzer, N.Y. Joly, G.K.L. Wong, A. Nazarkin, A. Podlipensky, M. Scharrer, P.St.J. Russell, Opt. Lett. **35**, 2922–2924 (2010)
22. R. Stolen, W. Leibolt, Appl. Opt. **15**, 239–243 (1976)
23. H.J. Lehmeier, W. Leupacher, A. Penzkofer, Opt. Commun. **56**, 67–72 (1985)
24. C. Bree, A. Demircan, G. Steinmeyer, IEEE J. Quant. Electron. **46**, 433–437 (2010)
25. G.P. Agrawal, *Nonlinear Fiber Optics*, 4th ed. (Academic Press, 2007)
26. A. Couairon, E. Brambilla, T. Corti, D. Majus, O. Ramírez-Góngora, M. Kolesik, Eur. Phys. J. Special Top **199**, 5–76 (2011)
27. V.P. Kandidov, V.Y. Fedorov, O.V. Tverskoy, O.G. Kosareva, S.L. Chin, Quantum Electron. **41**, 382–386 (2011)